

## Optical manifestation of magnetic polarons bound to excitons and resident holes in a (Cd,Mn)Te quantum well

N. V. Kozyrev <sup>\*</sup>, R. R. Akhmadullin , B. R. Namozov, and Yu. G. Kusrayev  
*Ioffe Institute, Russian Academy of Sciences, 194021 St. Petersburg, Russia*

G. Karczewski

*Institute of Physics, Polish Academy of Sciences, PL-02668 Warsaw, Poland*

T. Wojtowicz

*International Research Centre MagTop, Institute of Physics, Polish Academy of Sciences, PL-02668 Warsaw, Poland*



(Received 25 May 2021; accepted 7 July 2021; published 19 July 2021)

Photoluminescence and multiple  $\text{Mn}^{2+}$  spin-flip Raman scattering (SFRS) are studied in the (Cd,Mn)Te/(Cd,Mg)Te quantum well with excess resident hole concentration under resonance continuous-wave photoexcitation in the localized states of excitons and trions at  $T = 1.5$  K. A magnetic polaron shift of both exciton and trion photoluminescence is observed to be increasing with an increase in the magnetic field up to 6 T applied perpendicularly to the sample growth axis (Voigt geometry). Exciton magnetic polaron shift in magnetic field is attributed to the adiabatic energy transfer from the exchange reservoir to the Zeeman reservoir during the precession of the  $\text{Mn}^{2+}$  ions in the summary field of external magnetic and exchange hole fields. A mechanism of the magnetic polaron shift of trion photoluminescence is suggested. It is related to direct photoexcitation of the triplet trion state, which is stable in the conditions which are provided by the resident hole magnetic polarons. In these conditions, the  $\text{Mn}^{2+}$  magnetic moment experiences additional magnetization in the double exchange field provided by two holes in the triplet trion state. It is observed that the maximum efficiency of multiple  $\text{Mn}^{2+}$  spin-flip Raman scattering falls into the energy range corresponding to the states of localized excitons where the exciton magnetic polaron shift is observed. From this we conclude that the magnetic polaron state could be an intermediate state of the multiple  $\text{Mn}^{2+}$  SFRS process.

DOI: [10.1103/PhysRevB.104.045307](https://doi.org/10.1103/PhysRevB.104.045307)

### I. INTRODUCTION

Strong exchange interaction between magnetic ions and charge carriers (electrons or holes) leads to the manifestation of many phenomena observed in diluted magnetic semiconductors (DMSs) such as (Cd,Mn)Te and quantum structures based on them. One of these phenomena is the giant spin splitting of exciton states which can be observed in the photoluminescence (PL), absorption, and reflection spectra (e.g., Refs. [1,2]). This can be described as the influence of an effective exchange field produced by the localized spins of manganese ions on the spin of a charge carrier (or spins of the electron and the hole in an exciton). This exchange field acts as a magnetic field, and its value can easily exceed that of the usual external magnetic fields used in experiments (about 1 T) by one or two orders of magnitude. On the other hand, a band charge carrier (or an exciton itself) can create an exchange field, which would align spins of magnetic ions. The dynamics of this process is accompanied by spatial localization of the carrier (exciton) due to the exchange interaction with localized magnetic ions. This is known as the formation of a free (self trapped) magnetic polaron: a self-consistent bound state of

a charge carrier (or an exciton) and magnetic ions in the carrier (exciton) localization area [2]. However, free magnetic polaron formation is hardly achieved in two-dimensional systems [3]. There is another kind of magnetic polaron which is easier to observe: the bound magnetic polaron, which requires initial localization of the charge carrier (exciton) on imperfections of a semiconductor structure. This localization causes a significant enhancement of the exchange field of the charge carrier (exciton) and facilitates the possibility of the magnetic polaron formation. Hereinafter, we discuss only bound magnetic polarons and will refer to them just as magnetic polarons.

Several types of magnetic polarons are known so far. Among them is the exciton magnetic polaron (EMP), which originates due to the exchange interaction between the exciton (electron and hole) and the magnetic ions in its localization area. An EMP typically manifests itself as an additional energy shift of the exciton PL under resonant continuous-wave excitation in the low-energy tail of the density of states of the localized excitons in the bulk DMS [4] and in the DMS-based quantum structures [5]. In addition, the dynamic process of the EMP formation causes a time-dependent shift of the exciton PL spectral position, which can be researched by detecting the PL kinetics with time and energy resolution with a streak camera [6]. Another type is the electron or the hole magnetic polaron (EIMP or HMP, respectively), which forms in the

<sup>\*</sup>kozyrev.nikolay@bk.ru

vicinity of only one type of charge carrier—electron or hole, respectively. Charge carriers involved in the formation of such polarons can be either resident or bound to impurities. Spin dynamics of such HMPs were studied lately in the (Cd,Mn)Te quantum well (QW) [7] and in the (Cd,Mn)Te bulk [8] by means of the time-resolved pump-probe Kerr rotation technique. It was found that the spin lifetime of such HMPs in the QW is about 100 ns, which is several orders of magnitude higher than the typical spin relaxation times of charge carriers in that system ( $\sim 1\text{--}10$  ps).

Apart from the described phenomena the exchange interaction between magnetic ions and charge carriers also manifests itself in light-scattering processes. In particular, spin-flip Raman scattering (SFRS) in the (Cd,Mn)Te QW usually shows many (up to 19 in specific cases [9]) equidistant lines in the secondary emission spectra in a transverse magnetic field. These lines are related to the simultaneous spin flips of multiple magnetic ions. It is assumed that this phenomenon is connected to the participation of the virtual magnetic polaron state in the SFRS process [9,10], although the detailed mechanism of this process has not been proposed yet. Along with that, in papers related to the study of magnetic polarons, consideration of the multiple manganese SFRS process is almost always omitted [5,11]. One may suggest that the role of the magnetic polaron is to correlate the spins of the manganese ions in order to increase the probability of their simultaneous flip. Therefore it is necessary to consider the magnetic polaron's formation process along with the multiple manganese spin flips in the transversal magnetic field.

In this paper we study the role of the exciton magnetic polaron and the resident hole magnetic polaron in the formation of the secondary radiation spectra (PL and SFRS) in a (Cd,Mn)Te quantum well doped with resident holes, by means of selective photoexcitation with cw laser radiation.

The presentation order is the following: in Sec. II we briefly describe the growth process of the studied structure and the experimental technique. Experimental results of the resonant PL in the longitudinal and transversal magnetic fields and the SFRS are presented in Sec. III and discussed in Sec. IV. A summary and conclusions are given in Sec. V.

## II. EXPERIMENTAL DETAILS

The studied structure consisted of three  $\text{Cd}_{0.96}\text{Mn}_{0.04}\text{Te}$  DMS QWs with 40, 60, and 100 Å widths separated by a  $\text{Cd}_{0.76}\text{Mg}_{0.24}\text{Te}$  nonmagnetic barrier with 300 Å width grown by the molecular-beam epitaxy technique on a GaAs (001) substrate. In the QW with 40 Å width an excess resident hole concentration is present, which is confirmed by preliminary studies of that structure by means of the time-resolved pump-probe technique [7] and optically detected magnetic resonance investigation of a very analogous structure with 1% of molar manganese content ( $\text{Cd}_{0.99}\text{Mn}_{0.01}\text{Te}$ ) [12].

The sample was immersed in liquid helium cooled to 1.5 K in a cryostat with a superconductive split-coil magnet with magnetic field  $B$  up to 6 T. The optical axis was always directed along the growth axis of the sample. The direction of the magnetic field was either along the sample growth axis (longitudinal field, Faraday geometry) or perpendicular to it (transverse field, Voigt geometry). A tunable cw titanium-

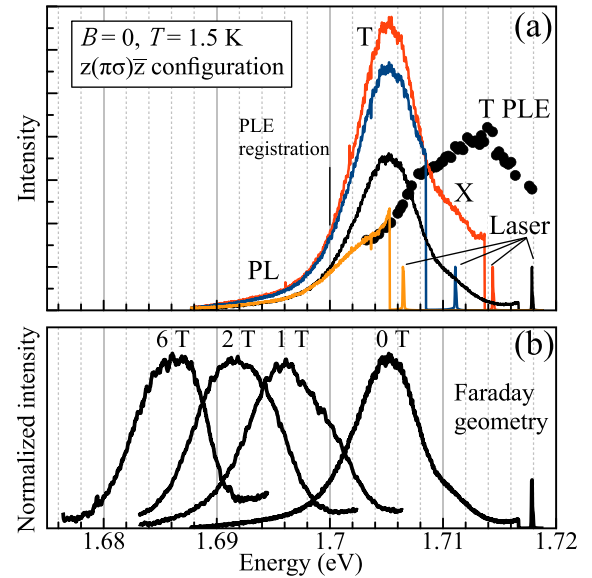


FIG. 1. (a) Colored curves represent resonant PL spectra under different photoexcitation energies in  $B = 0$ . Black circles represent the trion PLE spectrum registered at 1.701 eV (T PLE). Letters “T” and “X” denote the position of the trion and exciton PL, respectively. (b) Normalized PL spectra are presented at different magnetic fields in the Faraday geometry under photoexcitation with energy that is higher than the PL maxima by 10–15 meV.  $T = 1.5$  K.

sapphire laser with spectral width of about  $0.1 \mu\text{eV}$  was used as the source of the photoexcitation. The power density of the photoexcitation was kept constant with a value of about  $0.5 \text{ W}/\text{cm}^2$ , which caused minimal heating of the sample. Resonance PL spectra and multiple manganese SFRS registered with a triple Raman spectrometer with a spectral resolution of  $50 \mu\text{eV}$  and a CCD camera. During the investigation of PL and SFRS spectra in Voigt geometry, polarization of the incident and the registered light was taken to be linear: parallel or perpendicular to the magnetic field vector,  $\pi$  and  $\sigma$ , respectively. In this paper, spectra of the resonance PL and SFRS are detected in the  $z(\pi\sigma)\bar{z}$  configuration, which means  $\pi$ -polarized photoexcitation propagating along the growth axis ( $z$  axis) and detection of the  $\sigma$ -polarized secondary radiation detected along  $\bar{z}$ .

## III. EXPERIMENTAL RESULTS

### A. PL in $B = 0$ and in Faraday geometry

PL spectra of the QW with 40 Å width measured under resonant excitation in  $B = 0$  are shown in Fig. 1(a) as solid curves. One can see a single Gaussian-shaped PL contour with maximum at 1.705 eV attributed to the formation of the hole trion: the bound state of the exciton with the resident hole. On the high-energy side of the trion PL near 1.712 eV, a little shoulder can be seen, which is due to exciton recombination. Photoexcitation of the trions is the most efficient in the energy range between 1.706 and 1.716 eV, which overlaps with the spectral range of the trion and exciton states in the QW. The maximum at 1.714 eV and a feature at 1.708 eV observed in the trion photoluminescence excitation (PLE) spectrum [Fig. 1(a)] are ascribed to the maximum efficiency of the

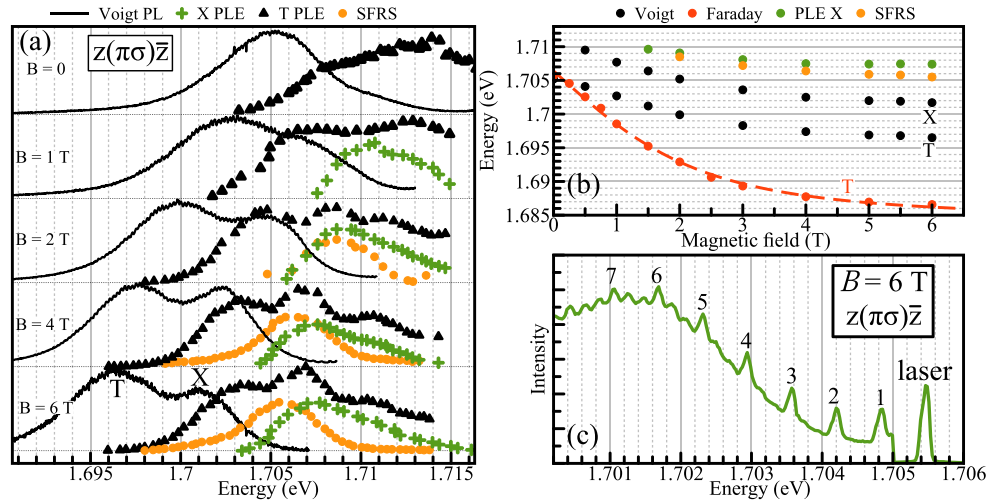


FIG. 2. (a) Black curves represent PL spectra registered under photoexcitation with the energies that are higher than trion PL maxima by 10–15 meV in different magnetic fields in the Voigt geometry. Black triangles and green pluses represent trion and exciton PLE spectra, respectively, and orange circles represent manganese SFRS resonance contours in different magnetic fields in the Voigt geometry. All spectra are obtained at the  $z(\pi\sigma)\bar{z}$  configuration, normalized and shifted vertically for clarity; horizontal dashed lines correspond to the zero intensity for each magnetic field. Letters “T” and “X” denote trion and exciton PL, respectively. (b) Magnetic field dependencies of the spectral positions of trion PL (red “T”) in the Faraday geometry (red circles) and of the exciton (black “X”) and the trion (black “T”) in the Voigt geometry (black circles); green circles represent the magnetic field dependence of the spectral position of the exciton PLE spectra maximum (PLE X), and orange circles represent the spectral position of the SFRS resonance contour maximum. The red dashed curve is the calculation of the giant Zeeman effect with the formula (1). (c) SFRS spectrum in  $B = 6$  T in Voigt geometry with an energy of excitation photons of 1.7055 eV. All data are presented for  $T = 1.5$  K.

exciton and trion absorption, respectively. The Stokes shift of the trion and exciton PL lines relative to the PLE spectra is due to the localization and inhomogeneous broadening of exciton and trion states in the QW.

Applying the magnetic field in Faraday geometry, one can observe a monotonic shift of the trion PL towards low energies [Figs. 1(b) and 2(b)]. We could not resolve exciton PL in Faraday geometry in the background of wider and stronger trion PL. The magnetic field dependence of the trion PL spectral position corresponds to the giant Zeeman effect typical for DMSs [1]

$$E_Z = E_0 - \frac{1}{2}(E_{Z,e} + E_{Z,hh})$$

$$= E_0 - \frac{1}{2}x_{Mn}N_0(\alpha - \beta)\langle S \rangle(B, T_{\text{eff}}). \quad (1)$$

Here,  $E_0$  is the spectral position of the PL in  $B = 0$ ,  $x_{Mn}$  is the effective molar manganese content,  $N_0\alpha = 0.22$  eV and  $N_0\beta = -0.88$  eV are constants of exchange interaction of manganese with electrons and holes, respectively, in (Cd,Mn)Te;  $\langle S \rangle(B, T_{\text{eff}}) = S \cdot B_S(\mu g S B / k T_{\text{eff}})$  is an average spin of the manganese ions dependent on magnetic field  $B$  and the effective temperature of the manganese spin system  $T_{\text{eff}}$ , where  $\mu$  is the Bohr magneton,  $g = 2.0$  is the  $g$  factor of  $3d$  electrons localized on  $Mn^{2+}$  ions, and  $S = 5/2$  is the manganese spin.  $B_S(x) = \frac{2S+1}{2S} \coth(\frac{2S+1}{2S}x) - \frac{1}{2S} \coth(\frac{1}{2S}x)$  is the Brillouin function. The coefficient  $\frac{1}{2}$  before formula (1) corresponds to the Zeeman shift of one branch of the exciton doublet in Faraday geometry.

Fitting the magnetic field dependence of the trion PL in Faraday geometry with formula (1) [Fig. 2(c)], we have

defined values of  $x_{Mn} = 1.8\%$  and  $T_{\text{eff}} = 3.5$  K. The latter corresponds to the temperature of the manganese spin system. It exceeds the sample temperature  $T = 1.5$  K because of the antiferromagnetic interaction between nearest-neighboring manganese ions. This interaction also leads to a decrease in the effective manganese content in DMSs in the not-so-diluted regime ( $x_{Mn} > 0.1\%$ ) [13]. Along with that,  $x_{Mn}$  may differ from the technological value of 4% because of some uncertainty in the determination of the manganese content during the growth process.

## B. PL and SFRS in Voigt geometry

Presented with solid black curves in Fig. 2(a) are PL spectra detected in different magnetic fields in Voigt geometry in the  $z(\pi\sigma)\bar{z}$  configuration. As one can see, application of the magnetic field in Voigt geometry also leads to the shift of the trion PL towards low energies. In  $B > 0.5$  T, one can observe a clear manifestation of the exciton PL in the spectra on the high-energy side with respect to trion PL. The exciton PL shape appears to be Gaussian. The spectral difference between exciton and trion PL maxima is about 6 meV and practically does not depend on magnetic field value. The spectral shift of both trion and exciton PL in the transverse magnetic field differs from formula (1) (and thus the Brillouin function) because of the hole spin anisotropy in QWs [14]. In Voigt geometry the state of the exciton formed by an electron and a heavy hole (the ground exciton state) is split into a quartet of states. One pair of these is  $\sigma$  polarized, and the other pair is  $\pi$  polarized. The energy difference between the former and the latter pairs is defined as a sum and a difference of electron and hole energy shifts in the magnetic field, respectively [14,15].

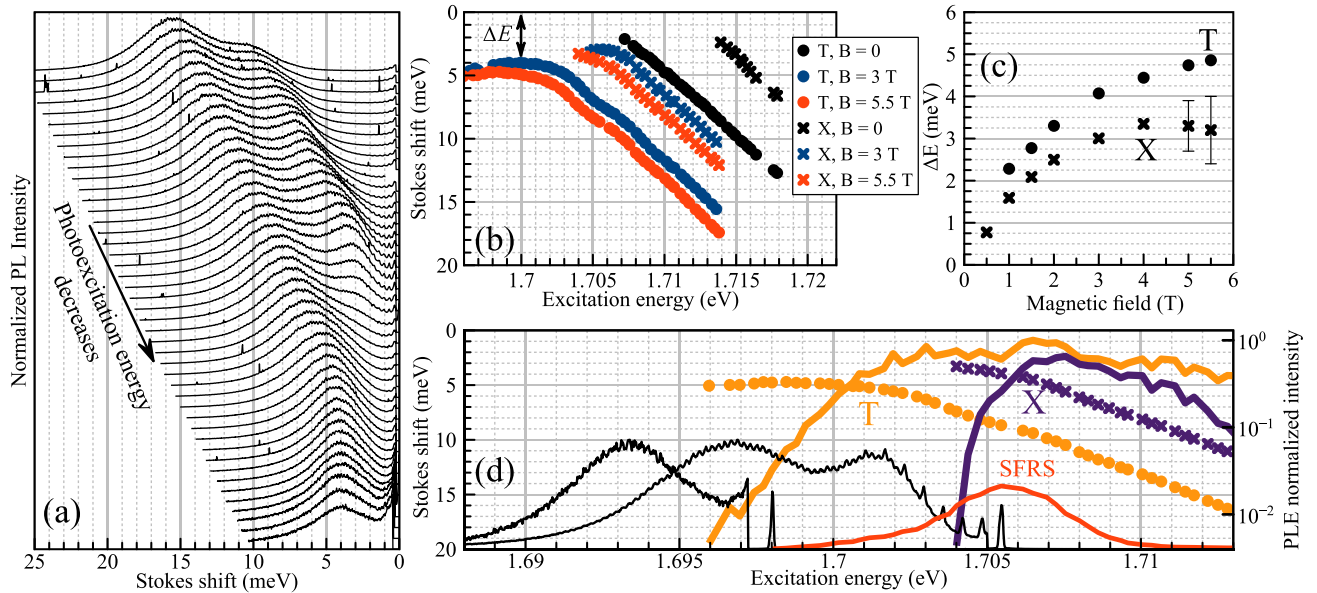


FIG. 3. (a) Secondary radiation spectra under resonant photoexcitation (energy of the laser decreases from the upper spectrum to the lower one) in  $B = 5.5$  T (Voigt) at  $T = 1.5$  K registered in the  $z(\pi\sigma)\bar{z}$  configuration. Spectra are normalized and shifted vertically for clarity. (b) Stokes shift of the exciton (X) and trion (T) PL over photoexcitation energy.  $\Delta E$  is a value of the constant Stokes shift in the magnetic field (clarification in text). (c) Magnetic field dependence of  $\Delta E$  for trion and exciton in Voigt geometry. (d)  $B = 5.5$  T,  $T = 1.5$  K. Orange and purple curves represent PLE spectra of the trion and exciton, respectively (right axis, log scale). Orange circles and purple crosses represent the spectral positions of the trion and exciton PL lines, respectively, for different photoexcitation energies (left axis). The red curve represents the normalized resonance contour of the manganese SFRS, and black curves represent PL spectra at the excitation with  $E = 1.7055$  eV corresponding to the exciton state and with  $E = 1.698$  eV, which is in the trion localized state's spectral range. The latter curves are on a linear scale and are not linked to any ordinate axis.

In  $B = 6$  T, the linear polarization degree of the exciton and trion PL reaches 80%, which is apparently connected to the splitting of the heavy hole states in the transverse field (about 2 meV), which is much more than the thermal energy in  $T = 1.5$  K (0.13 meV).

Since in the transverse magnetic field we were able to distinguish between exciton and trion PL, we have fitted spectra with two Gaussian curves in order to establish the intensity and spectral position of both of them separately. In each magnetic field we measured a series of PL spectra at different excitation energies [an example of such a series is shown in Fig. 3(a)]. Then we deduced exciton and trion PLE spectra as a dependence of the corresponding Gaussian amplitudes on the photoexcitation energy [see Fig. 2(a)]. In  $B > 1$  T, exciton PLE spectra form a clear resonance contour, whose asymmetrical shape might be due to the overlapping of two unresolved  $\pi$ -polarized exciton states. Therefore the maximum of exciton PLE spectra is attributed to the lowest of these two states. The energy between maxima of the exciton PL and PLE spectra increases with the magnetic field, which can be seen in Figs. 2(a) and 2(b).

As one can see in Fig. 2(a), features at 1.708 and 1.714 eV observed in the trion PLE spectrum in  $B = 0$  preserve their structure in the magnetic field in Voigt geometry. The former feature evolves into a distinct maximum shifting towards low energies with increasing transverse magnetic field. This corresponds to the direct excitation to the trion state in the QW. The high energy maximum observed in  $B = 0$  splits into two states in the transversal magnetic field. The shift of these with increasing  $B$  is practically the same as the shift of the

exciton PLE spectrum; therefore we suggest that these are due to excitation of  $\pi$ -polarized excitons with subsequent trion formation. The close values of amplitudes of all three maxima in the trion PLE spectra might be pointing to a high efficiency of the trion formation process.

The set of narrow equidistant lines (up to seven) can be observed in the secondary radiation spectra in the transverse magnetic fields under resonant excitation [Fig. 2(c)]. These lines correspond to the multiple manganese SFRS and are typically observed in quantum structures based on DMSs (first reported in Ref. [9]). The resonance contour of the SFRS was taken as an intensity of the first SFRS line over the photoexcitation energy, and it was measured for  $B > 2$  T in  $z(\pi\sigma)\bar{z}$  [Fig. 2(a)]. With increasing magnetic field, the spectral position of the SFRS contour maximum shifts towards low energies relative to the exciton PLE spectrum [Figs. 2(a) and 2(b)]. In our opinion this shift is directly attributed to the participation of the magnetic polaron state as an intermediate state in the multiple manganese SFRS process [9]. As will be stated later, this conclusion is based on the experimental fact that the maximum efficiency of the multiple manganese SFRS process falls into the energy range corresponding to the tail of the localized exciton density of states. Direct photoexcitation in that range also leads to the manifestation of the magnetic polaron shift in the transversal magnetic field.

### C. Magnetic polaron shift in Voigt geometry

In transverse magnetic fields it was observed that if one scans the laser energy from high values towards the PL spec-

trum, then the energy difference between the laser line and the exciton or trion PL (referred to later on as the Stokes shift) reaches a constant value  $\Delta E$  when the laser passes a certain energy threshold [see Figs. 3(a) and 3(b)]. After that the exciton line vanishes very quickly from the PL spectrum, whereas for the trion this effect can be seen in a rather large energy range. As was noted in the Introduction this behavior of the exciton PL was observed in other experiments [5] in systems with much higher manganese content under resonant photoexcitation in  $B = 0$ . This energy shift, which does not depend on the energy of the excitation photons, is interpreted to be a consequence of a magnetic polaron formation. However, in our experiment the shift  $\Delta E$  arises only in a rather strong transverse magnetic field (in  $B = 0$  this shift is not clearly seen). For the exciton we ascribe this effect to the magnetic polaron formation in the transversal magnetic field due to the energy transfer to the Zeeman reservoir [11], which features we discuss in Sec. IV.

Figure 3(b) shows dependencies of the exciton and trion PL Stokes shift on the photoexcitation energy in different magnetic fields. In the absence of the magnetic field, neither the exciton PL position nor the trion PL position depends on the laser energy, and the Stokes shift dependence on the laser energy is linear with a proportionality coefficient of 1 and  $\Delta E = 0$ . With the increase in the transverse magnetic field this dependence deviates from linear, and the  $\Delta E$  value increases for both exciton and trion PL [see Fig. 3(c)]. As can be seen, the Stokes shift of the trion PL reaches a constant value over all of the range of the studied magnetic fields. On the other hand, the exciton PL Stokes shift dependence on the photoexcitation energy in  $B > 4$  T after passing the energy threshold just decreases the linearity coefficient rather than going to the constant value [see Fig. 3(b) for X in  $B = 5.5$  T]. This might be pointing to the effective decrease in  $\Delta E$  for the exciton with further increase in the magnetic field [11]. Since we cannot precisely define the  $\Delta E$  value for exciton PL in  $B > 4$  T, we put in Fig. 3(c) points corresponding to the mean value of the Stokes shift after the energy threshold with error bars representing the variance of the exciton Stokes shift in high fields.

Complementary analysis of the Stokes shift and the intensity of the exciton and trion PL has shown that the energy threshold after which the Stokes shift goes to the plateau corresponds to the energy of the photoexcitation where the PL intensity starts to decrease [see Fig. 3(d)]. The decrease in the intensity is apparently connected to the decrease in the exciton or trion density states. Therefore the energy threshold can be interpreted as the exciton mobility threshold [purple curve in Fig. 3(d)] or direct excitation of the localized trion states [orange curve in Fig. 3(d)].

## IV. DISCUSSION

### A. Exciton magnetic polaron shift $\Delta E$ in Voigt geometry

Manifestation of the exciton PL magnetic polaron shift under resonant photoexcitation of QWs based on a (Cd,Mn)Te DMS is caused by the fulfillment of two conditions. First of all, the following inequality is to be satisfied:

$$\tau_{\text{MP}} < \tau. \quad (2)$$

Here,  $\tau_{\text{MP}}$  and  $\tau$  are phenomenological times of magnetic polaron formation and the exciton lifetime, respectively. Essentially, this inequality is what underlies the fact that most excitons will form a magnetic polaron before recombination. The second condition of exciton magnetic polaron (EMP) formation in a two-dimensional (2D) quantum DMS system is that the exciton requires an initial localization [3]. New-born excitons could localize on imperfections of the structure caused by monolayer fluctuations of the QW width, deformation potential on heterointerfaces, or inhomogeneity of the composition. After that, the EMP can be formed, and during the formation process a further decrease in the exciton localization volume, up to two to three times, occurs due to the exchange interaction between the exciton and the manganese ions [16].

EMP formation, which often manifests itself in (Cd,Mn)Te QWs with high manganese content ( $x_{\text{Mn}} \sim 10\%$ ) in  $B = 0$  (see, e.g., Refs. [5,6,11]), does not seem to take place in our system even when we excite the system into the localized exciton states. This directly points to the large time of the EMP formation  $\tau_{\text{MP}}$  relative to the exciton lifetime, which is measured in this structure to be  $\tau = 100$  ps [7].

Application of the transverse magnetic field leads to the emergence of the distinct exciton PL and to the manifestation of the constant Stokes shift  $\Delta E$  (described in Sec. III C) when we excite the system into the localized exciton states. Although we cannot clearly describe the origin of the former effect, the latter one we attribute to EMP formation. We need to make a short remark: hereinafter in this section we intentionally discard the exchange interaction between the electron in the exciton and manganese ions from consideration. Firstly, its exchange constant is four times smaller than that of the heavy hole, and secondly, its spin is fully isotropic, which will not contribute any valuable information to the effect. The possibility of EMP formation in the transverse  $B$  is due to the effective shortening of  $\tau_{\text{MP}}$  occurring in the process proposed and thoroughly described in Ref. [11]. According to the mechanism of this process, most of the EMP energy is gained over the transversal spin relaxation time  $T_2$  of manganese ions during its precession around the total magnetic field  $\mathbf{B}_{\text{total}} = \mathbf{B} + \mathbf{B}_{\text{ex}}$ , where  $\mathbf{B}$  is the transversal external magnetic field and  $\mathbf{B}_{\text{ex}}$  is the exchange field of the heavy hole in the exciton. Because of the hole spin anisotropy in QWs,  $\mathbf{B}_{\text{ex}}$  and  $\mathbf{B}$  are not collinear. Due to strong inhomogeneity of the exchange field the Larmor frequency of the manganese spin precession has a large variance. Thus  $T_2$  becomes comparable to the Larmor precession period  $T_L = 2\pi\hbar/\mu gB$  ( $\hbar$  is the Plank constant). This time is 36 ns in  $B = 1$  T, which is more than two times less than  $\tau$ . Therefore in transverse  $B$  the inequality (2) is satisfied, and since we have also established initial localization of the excitons by appropriate choice of the photoexcitation energy, the EMP now can be formed. That originates the magnetic polaron shift of the exciton PL in a transversal magnetic field. The physical mechanism of the manganese magnetic moment precession in  $\mathbf{B}_{\text{total}}$  is rather versatile and finds application in the description of other phenomena observed in the DMSs. For example, it is used to describe the effect of the multiple manganese spin-flip Raman scattering in the DMS-based QWs [9,10], and it underlies the anomalous Hanle effect in the DMS-based QWs [17].

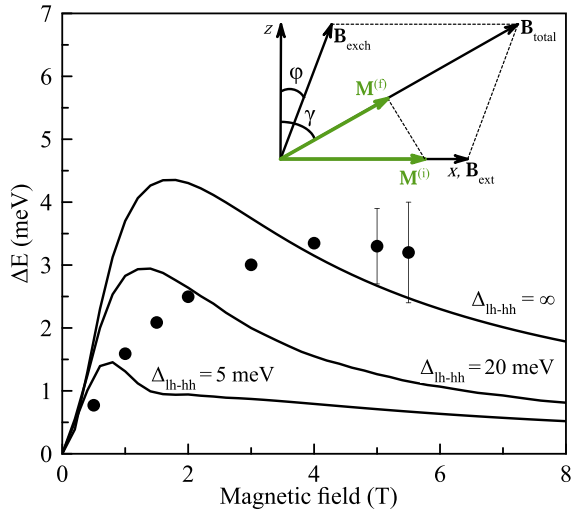


FIG. 4. Black circles represent the transverse magnetic field dependence of the EMP shift  $\Delta E$ . Black curves represent the calculation according to the model suggested in Ref. [11] with parameters  $x_{\text{Mn}} = 0.018$ ,  $T_{\text{eff}} = 3.5$  K, and  $B_{\text{ex}} = 0.8$  T and different values of the  $\Delta_{\text{lh-hh}}$  parameter (the curve with  $\Delta_{\text{lh-hh}} = \infty$  corresponds to  $\varphi = 0$  in all  $B$ ).

The value of the magnetic polaron shift appearing in the transversal magnetic field due to the mechanism described in Ref. [11] can be calculated by solving the self-consistent problem of finding the energy of the following system: in this system,  $\text{Mn}^{2+}$  magnetic moments are subjected to  $\mathbf{B}_{\text{total}}$ , and heavy hole spin is subjected to the exchange field of manganese ions (the influence of the external magnetic field on the hole is not considered because of its smallness compared with the exchange field of manganese), which tries to incline the hole spin from the growth axis. This is shown schematically in Fig. 4. Before the photoexcitation the magnetic moment of manganese ions  $\mathbf{M}^{(i)}$  is directed along the magnetic field axis. After the exciton is born this net manganese magnetic moment in the exciton localization volume starts to precess around  $\mathbf{B}_{\text{total}}$  and quickly (by the time  $T_2$  defined earlier) dephases, which can be interpreted as a projection of  $\mathbf{M}^{(i)}$  on the  $\mathbf{B}_{\text{total}}$  axis. Therefore the absolute value of the manganese ions' magnetic moment in the final state is  $|\mathbf{M}^{(f)}| = |\mathbf{M}^{(i)}| \cdot \sin \gamma$ , where angle  $\gamma$  defines the direction of  $\mathbf{B}_{\text{total}}$  (and thus  $\mathbf{M}^{(f)}$ ). On the other hand, angle  $\gamma$  itself depends on the inclination of the heavy hole exchange field from the  $z$  axis (angle  $\varphi$ ).

The formal procedure of solving this problem is described in Ref. [11] and includes three parameters: the Zeeman splitting of the heavy hole state in the longitudinal magnetic field ( $E_{Z,\text{hh}}$ ), which is defined from the experiment; the value  $\Delta_{\text{lh-hh}}$  defining splitting between light and heavy holes in the quantum well (this parameter defines the mixture between light and heavy hole states and therefore the dependence of the angle  $\varphi$  on  $B$ ); and the heavy hole exchange field  $B_{\text{ex}}$  in the exciton magnetic polaron. The latter we estimate to be 0.8 T with the formula suggested in Ref. [18], which includes an experimentally defined derivation of the Zeeman shift and circular polarization degree of PL on the magnetic field in Faraday geometry in the vicinity of  $B = 0$ . This parameter is defined in the ‘‘exchange box’’ approximation, in which

the exchange field is considered to be constant in the exciton localization volume and to be zero outside it. This approximation is commonly used and often leads to good agreement with the experimental results. In our discussion we take  $\Delta_{\text{lh-hh}}$  as a free parameter. The result of the calculation along with the experimental results of the exciton  $\Delta E$  value are shown in Fig. 4.

Basically, the EMP shift is proportional to the energy of the exchange interaction between  $\text{Mn}^{2+}$  and the heavy hole, which is defined by the dot product  $\mathbf{B}_{\text{ex}} \cdot \mathbf{M}$ . With the increase in the transverse magnetic field, the EMP shift grows and reaches maximum, which follows the increase and saturation of the manganese magnetic moment. With further increase in the magnetic field, the EMP shift decreases because the angle  $\gamma$  between  $\mathbf{B}_{\text{ex}}$  and  $\mathbf{M}^{(f)}$  increases up to  $90^\circ$ , where the projection of the manganese spin on the heavy hole exchange field is zero and EMP is not formed. Smaller values of  $\Delta_{\text{lh-hh}}$  mean that the heavy hole spin is more influenced by the manganese exchange field and is more inclined from the growth axis ( $\varphi$  has a stronger dependence on  $B$ ). Thus the maximum of the EMP shift is reached in lower magnetic fields, and processes of the EMP suppression are to be taken into account.

One can see that the model suggested in Ref. [11] adequately describes the qualitative behavior of the EMP shift in our structure even in the infinite-anisotropy approximation, where heavy hole spin is directed along the growth axis and  $\Delta_{\text{lh-hh}} = \infty$  ( $\varphi$  is always zero). Namely, all tendencies are observed in the experiment: the EMP shift grows with the magnetic field, reaches maximum, and then decreases with further increase in the magnetic field. However, even with  $\Delta_{\text{lh-hh}} = \infty$  the calculated EMP shift reaches maximum at magnetic fields that are two times lower than those at which the experimental EMP shift reaches maximum (decrease in the effective EMP occurs after 4 T). This mismatch can happen for three reasons. First of all, we do not take into account the longitudinal manganese spin relaxation time  $T_1$  on the  $\mathbf{B}_{\text{total}}$  in our calculation. Although the  $T_1$  of manganese is much longer than  $T_2$ , it can also play a certain role in the EMP shift derivation because it is responsible for the increase in the  $\mathbf{M}^{(f)}$  vector length. Secondly, we define the heavy hole  $B_{\text{ex}}$  parameter in the exchange box approximation, whereas in real life the exchange field value is different for different points in space, which apparently is to be considered. Last but not least, in this model,  $B_{\text{ex}}$  is taken to be constant; however, during the process of the EMP formation an additional localization of the exciton volume takes place. This, in turn, leads to the gradual increase in the exchange field of the heavy hole over time, which also should be considered.

## B. Energy shift $\Delta E$ of trion PL in Voigt geometry

Along with the exciton magnetic polaron shift, the trion PL line also manifests the Stokes shift going to the constant value  $\Delta E$  when the laser energy reaches a certain threshold. As for EMP, its shift occurs due to the change in the average manganese magnetic moment projection on the  $\mathbf{B}_{\text{ex}}$  from zero to a finite value. As for the trion, it consists of a photoexcited exciton and a resident hole in a QW, which has an infinite lifetime, and by the moment of photoexcitation a hole magnetic polaron (HMP) is already formed. Therefore the average

manganese magnetic moment initially has nonzero projection on the  $\mathbf{B}_{\text{ex}}$ , and thus the trion  $\Delta E$  shift must have another origin.

Usually, trions are considered to be excited in the singlet state (see, e.g., Ref. [7]). In the case of a singlet, the trion consists of an electron and two holes with opposite spins which do not participate in the exchange interaction with the manganese ions. The photoexcited electron in the singlet trion finds itself in the excited state of the giant Zeeman doublet due to the interaction with manganese. Consequently, the electron spin flips, and after trion recombination the radiated photon will be red shifted with respect to the incident one. The  $\Delta E$  shift of the singlet trion PL then will be as much as a giant Zeeman splitting of the electron state. In our experiments, in  $B = 6$  T the former is nearly two times larger than the  $\Delta E$  shift of trion PL. Having this quantitative disagreement, we suggest another scenario.

For simplicity we consider that the heavy hole exchange field is always directed along the growth axis (i.e., the infinite-anisotropy approximation). As was noted earlier, manganese ions involved in the HMP formation create their own exchange field acting on the heavy hole spin and stabilizing it. The value of the manganese exchange field  $B_{\text{Mn}}$  can be estimated by rewriting the magnetic polaron energy via the giant Zeeman splitting as

$$\frac{1}{2}E_{Z,\text{hh}}(B_{\text{ex}}) = \mu g_{\text{hh}} J B_{\text{Mn}}. \quad (3)$$

Here,  $E_{Z,\text{hh}}(B_{\text{ex}})$  is the heavy hole giant Zeeman splitting in Faraday geometry taken in the heavy hole exchange field (i.e., the magnetic polaron energy). On the right side of the equation it is written how the manganese exchange field acts on the heavy hole spin  $J = 3/2$  with  $g_{\text{hh}}$ : the  $g$  factor in pure CdTe. Taking  $B_{\text{ex}} \approx 1$  T, one obtains  $E_{Z,\text{hh}}(B_{\text{ex}})$  about 14 meV from the PL shift. If now one takes  $g_{\text{hh}} \approx 1$ , one will have  $B_{\text{Mn}} \approx 80$  T. With such values of the effective magnetic field of manganese acting on a hole the ground state of the hole trion should be triplet. This conclusion is supported by the study of nonmagnetic CdTe/(Cd,Mg)Te QWs subjected to external magnetic fields up to 45 T [19]. Therefore tuning the energy of the photons to the range of the direct trion photoexcitation where the hole is in the HMP [as, e.g., below the 1.701 eV in  $B = 5.5$  T; Fig. 3(d)], one would have the following situation: since the excited trion is in the triplet state, the spins of both holes point in the same direction. Essentially, this means that the manganese ions in the HMP are subjected to the double heavy hole exchange field after trion photoexcitation.

The value  $\Delta E$  for the trion PL shift in the transversal magnetic field can be estimated as a difference between energies of the system before the photoexcitation  $E_i$  (initial) and after trion recombination  $E_f$  (final). In the initial state, the manganese magnetic moment is subjected to the total magnetic field  $\mathbf{B}_{\text{total}}^{(i)} = \mathbf{B}_{\text{ex}} + \mathbf{B}$ , and the energy of the system is defined as

$$E_i = \mathbf{B}_{\text{ex}} \cdot \mathbf{M}(\mathbf{B}_{\text{total}}^{(i)}, T_{\text{eff}}). \quad (4)$$

After a trion is photoexcited in the triplet state the manganese magnetic moment is defined by  $\mathbf{B}_{\text{total}}^{(f)} = 2\mathbf{B}_{\text{ex}} + \mathbf{B}$ . After trion recombination the electron and one of the holes

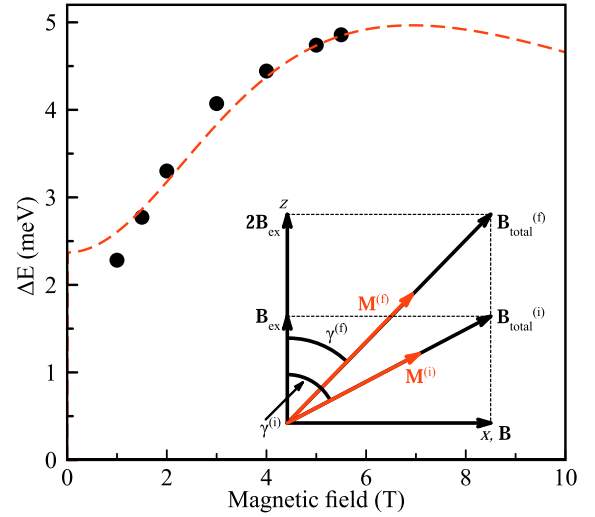


FIG. 5. Value  $\Delta E$  for trions (black circles) and the calculation of the model of the additional magnetization of manganese ions when the triplet trion state is excited (red dashed curve). On scheme  $\mathbf{M}^{(i,f)} = \mathbf{M}(\mathbf{B}_{\text{total}}^{(i,f)}, T_{\text{eff}})$ .

disappear, and the manganese magnetic moment finds itself in a nonequilibrium state as though it were still in  $\mathbf{B}_{\text{total}}^{(f)}$ . However, since there is only one hole exchange field to interact with, the energy of the final state is written as

$$E_f = \mathbf{B}_{\text{ex}} \cdot \mathbf{M}(\mathbf{B}_{\text{total}}^{(f)}, T_{\text{eff}}). \quad (5)$$

This is shown schematically in Fig. 5. In the “quantum box” approximation the hole exchange field is written as  $\mathbf{B}_{\text{ex}} = \mathbf{e}_z \beta J / 3 \mu g V$ , where  $V$  is the heavy hole localization volume and  $\mathbf{e}_z$  is the unit vector along the  $z$  axis. On the other hand, the magnetic moment of manganese ions is written as  $\mathbf{M}(\mathbf{B}, T_{\text{eff}}) = \mathbf{e}_{\mathbf{B}} x_{\text{Mn}} \mu g N_0 V \langle S \rangle (\mathbf{B}, T_{\text{eff}})$ , where  $\mathbf{e}_{\mathbf{B}}$  is the unit vector in the direction of the magnetic field  $\mathbf{B}$  acting on manganese.

Localization volumes, Bohr magnetons, and  $g$  factors of manganese cancel each other out, and taking into account dot products in formulas (4) and (5), the energy can be rewritten as

$$E_{i,f} = \frac{1}{2} \beta N_0 x_{\text{Mn}} \langle S \rangle (|\mathbf{B}_{\text{total}}^{(i,f)}|, T_{\text{eff}}) \cos \gamma^{(i,f)}. \quad (6)$$

Here, angles  $\gamma^{(i,f)}$  are taken between the  $z$  axis and  $\mathbf{B}_{\text{total}}^{(i,f)}$  for the initial and the final state, respectively. In this formula the part  $\beta N_0 x_{\text{Mn}} \langle S \rangle (|\mathbf{B}_{\text{total}}^{(i,f)}|, T_{\text{eff}})$  closely resembles giant Zeeman splitting of the heavy hole in Faraday geometry taken in the total magnetic field in the initial or the final state, respectively, and therefore can be rewritten in a very simple form

$$E_{i,f} = \frac{1}{2} E_{Z,\text{hh}} (|\mathbf{B}_{\text{total}}^{(i,f)}|, T_{\text{eff}}) \cos \gamma^{(i,f)}. \quad (7)$$

In the suggested approach for the trion magnetic polaron shift a magnetization of the manganese ions occurs in the exchange field of the heavy hole, which is also true for the exciton magnetic polaron formation. However, the  $\Delta E$  shift for triplet trion PL arises due to additional manganese magnetization from nonzero projection of  $\mathbf{M}$  on  $\mathbf{B}_{\text{ex}}$  in contrast

to the EMP shift, where initially (right after photoexcitation)  $\mathbf{M} \cdot \mathbf{B}_{\text{ex}} = 0$ .

The difference between  $E_i$  and  $E_f$  in formula (7) basically gives the change in energy of a resident hole in the HMP in the process of additional manganese magnetization. In order to complete the argumentation and proceed to the calculation, one needs to take into account a change in the energy of the electron present in the trion. Since the electron spin is isotropic, it follows the manganese magnetization during the whole process. Therefore formula (7) is to be supplemented with the giant Zeeman splitting of the electron  $E_{Z,e}$  in corresponding states:

$$E_{i,f} = \frac{1}{2} [E_{Z,h}(|\mathbf{B}_{\text{total}}^{(i,f)}|, T_{\text{eff}}) \cos \gamma^{(i,f)} + E_{Z,e}(|\mathbf{B}_{\text{total}}^{(i,f)}|, T_{\text{eff}})]. \quad (8)$$

With this we can now calculate the change in energy  $E_i - E_f$  taking into account both electron and hole change in energy during the process of manganese magnetization. The fit parameters of this model are  $\chi_{\text{Mn}}$  and  $T_{\text{eff}}$ , present in the giant Zeeman splitting of both charge carriers, whose exact values we took from the magnetic field dependence of the PL shift in Faraday geometry, and  $B_{\text{ex}}$ , which we set as a free parameter. In Fig. 5 a comparison between the experimental value  $\Delta E$  for trion PL and the calculation is presented. Good agreement is achieved with the rather surprising value of  $B_{\text{ex}} = 3.7$  T. Such a high value of the hole exchange field compared with the 0.8 T estimated earlier can be explained by the following: as was mentioned earlier, a resident hole has an infinite lifetime and can form a magnetic polaron in the equilibrium state. That is, the hole in the HMP has a very localized wave function due to the exchange interaction with manganese ions. On the other hand, the photogenerated exciton has to spend some time ( $\tau_{\text{MP}}$ , on average) to reach the equilibrium. Over this time the exciton localization volume decreases, and  $B_{\text{ex}}$  increases. However, since inequality (2) does not seem to hold in our system, the EMP does not reach the equilibrium state, and therefore its  $B_{\text{ex}}$  is smaller.

Although the localization volume of the hole in the equilibrium ( $B_{\text{ex}} = 3.7$  T) should be small, the hole wave function does not collapse. The volume could be estimated as  $V = \beta J / 3\mu g B_{\text{ex}}$  with a value of about  $70 \times 10^3 \text{ \AA}^3$ . The radius of that volume is 23 Å with the 40 Å QW width, and about 15 manganese ions fall into that volume.

Even though these simple arguments allow one to gain a precise enough agreement with experiment (Fig. 5), we must confess here that we did not consider the dynamics of the process of additional manganese ions' magnetization. In other words, to follow the process of the triplet trion magnetic polaron shift consistently, one needs first to consider

the manganese precession around  $\mathbf{B}_{\text{total}}^{(f)}$  and use the arguments discussed in Sec. IV A. However, this alone could not give us quantitative agreement between the experimental results and the calculation. In order to have our arguments work, we had to assume that both spin and energy relaxation of the manganese magnetic moment in the total magnetic field in the final stage of the process is completely finished before the trion recombination. This is not obvious, and moreover, in Sec. IV A we pointed out that the longitudinal relaxation time  $T_1$  of manganese is much longer than the exciton lifetime. However, we suppose that in conditions which the HMP provides—strong localization and high exchange field of the hole—the shortening of the manganese spin and energy relaxation times occurs.

## V. CONCLUSIONS

In this paper the role of the magnetic polarons in the formation of the secondary radiation spectra is studied. Under quasisonant excitation in the transversal magnetic field a constant Stokes shift of exciton and trion PL is observed that does not depend on the photoexcitation energy. In the case of the excitons this effect is attributed to the fast acceleration of the magnetic polaron formation process due to the manganese precession around  $\mathbf{B}_{\text{total}}$  [11]. In the case of trions the origin of the effect is different in principle, and we suggest that the magnetic polaron formed with the resident hole provides conditions for the triplet trion state stabilization. Photogeneration of the triplet trion leads to the additional magnetization of the manganese ions in the doubled hole exchange field. This, in turn, originates the manifestation of the constant shift  $\Delta E$  of trion PL under resonant photoexcitation. It was observed that the multiple manganese spin-flip Raman scattering process is the most effective in the range of the photoexcitation energies corresponding to the exciton magnetic polaron formation in the transversal magnetic field. This directly points to the connection between these two phenomena and to the possibility of the participation of the magnetic polaron state as an intermediate one in the SFRS process.

## ACKNOWLEDGMENTS

The authors thank K. V. Kavokin and S. A. Tarasenko for fruitful discussions and valuable advice. This work was supported by the RFBR (Project 19-52-12066) and DFG in the frame of the ICRC TRR 160 (Project B4). The research in Poland was partially supported by the Foundation for Polish Science through the IRA Programme cofinanced by the EU within SG OP (Grant No. MAB/2017/1).

- 
- [1] A. V. Komarov, S. M. Ryabchenko, O. V. Terletsii, I. I. Zheru, and R. D. Ivanchuk, *Zh. Eksp. Teor. Fiz.* **73**, 608 (1977) [*Sov. Phys. JETP* **46**, 318 (1977)].
- [2] J. K. Furdyna, *J. Appl. Phys. (Melville, NY)* **64**, R29 (1998).
- [3] C. Benoit á la Guillaume, *Phys. Status Solidi B* **175**, 369 (1993).

- [4] G. Mackh, W. Ossau, D. R. Yakovlev, A. Waag, G. Landwehr, R. Hellmann, and E. O. Gobel, *Phys. Rev. B* **49**, 10248 (1994).
- [5] D. R. Yakovlev, W. Ossau, G. Landwehr, R. N. Bicknell-Tassius, A. Waag, and I. N. Uraltsev, *Solid State Commun.* **76**, 325 (1990).
- [6] D. R. Yakovlev, W. Ossau, G. Landwehr, R. N. Bicknell-Tassius, A. Waag, S. Schmeusser, I. N. Uraltsev, A.



- Pohlmann, and O. E. Gøbel, *J. Cryst. Growth* **117**, 854 (1992).
- [7] E. A. Zhukov, Yu. G. Kusrayev, K. V. Kavokin, D. R. Yakovlev, J. Debus, A. Schwan, I. A. Akimov, G. Karczewski, T. Wojtowicz, J. Kossut, and M. Bayer, *Phys. Rev. B* **93**, 245305 (2016).
- [8] E. A. Zhukov, Yu. G. Kusrayev, E. Kirstein, A. Thomann, M. Salewski, N. V. Kozyrev, D. R. Yakovlev, and M. Bayer, *Phys. Rev. B* **99**, 115204 (2019).
- [9] J. Stühler, G. Schaack, M. Dahl, A. Waag, G. Landwehr, K. V. Kavokin, and I. A. Merkulov, *Phys. Rev. Lett.* **74**, 2567 (1995).
- [10] K. V. Kavokin and I. A. Merkulov, *Phys. Rev. B* **55**, R7371 (1997).
- [11] D. R. Yakovlev, K. V. Kavokin, I. A. Merkulov, G. Mackh, W. Ossau, R. Hellmann, E. O. Gøbel, A. Waag, and G. Landwehr, *Phys. Rev. B* **56**, 9782 (1997).
- [12] A. S. Gurin, D. O. Tolmachev, N. G. Romanov, B. R. Namozov, P. G. Baranov, Yu. G. Kusrayev, and G. Karczewski, *Pis'ma Zh. Eksp. Teor. Fiz.* **102**, 259 (2015) [*JETP Lett.* **102**, 230 (2015)].
- [13] W. J. Ossau and B. Kuhn-Heinrich, *Phys. B (Amsterdam)* **184**, 422 (1993).
- [14] B. Kuhn-Heinrich, W. Ossau, E. Bangert, A. Waag, and G. Landwehr, *Solid State Commun.* **91**, 413 (1994).
- [15] A. V. Koudinov, I. A. Akimov, Yu. G. Kusrayev, and F. Henneberger, *Phys. Rev. B* **70**, 241305(R) (2004).
- [16] D. R. Yakovlev, W. Ossau, A. Waag, R. N. Bicknell-Tassius, G. Landwehr, K. V. Kavokin, A. V. Kavokin, I. N. Uraltsev, and A. Pohlmann, in *Proceedings of the 21st International Conference on Physics of Semiconductors, Beijing, China, 1992* (World Scientific, Singapore, 1992), p. 1136–1139.
- [17] A. V. Koudinov, Yu. G. Kusrayev, I. A. Merkulov, K. V. Kavokin, I. G. Aksyanov, and B. P. Zakharchenya, *Fiz. Tverd. Tela* **45**, 1297 (2003) [*Phys. Solid State* **45**, 1360 (2003)].
- [18] I. A. Merkulov, G. R. Pozina, D. Coquillat, N. Paganotto, J. Siviniant, J. P. Lascaray, and J. Cibert, *Phys. Rev. B* **54**, 5727 (1996).
- [19] D. Andronikov, V. Kochereshko, A. Platonov, T. Barrick, S. A. Crooker, and G. Karczewski, *Phys. Rev. B* **72**, 165339 (2005).